J Fluoresc (2012) 22:511–519
DOI 10.1007/s10895-011-0985-1

ORIGINAL PAPER

Binding of Engeletin with Bovine Serum Albumin: Insights from Spectroscopic Investigations

Xialian Peng · Jing Yu · Qing Yu · Hedong Bian · Fuping Huang · Hong Liang

Received: 27 May 2011 / Accepted: 16 September 2011 / Published online: 27 September 2011

Abstract In this paper, several spectroscopic techniques were used to investigate the interaction of engeletin (ELN) with bovine serum albumin (BSA). The analysis of UV–Vis absorption and fluorescence spectra revealed that ELN and BSA formed a static complex ELN–BSA, and ELN quenched the fluorescence of BSA effectively. According to the thermodynamic parameters ΔS^0=47.27 J·mol^{-1}·K^{-1} and ΔH^0=−10.34 kJ·mol^{-1}, the hydrophobic and hydrogen bond interactions were suggested to be the major interaction forces between ELN and BSA. Raman spectroscopy indicated that the binding of ELN slightly changed the conformations and microenviroment of BSA and decreased the α–helix content of BSA.

Keywords Engeletin · BSA · UV–Vis absorption spectra · Fluorescence spectra · Raman spectra

Introduction

Engeletin (ELN), dihydrokaempferol 3-O-α-L-rhamnoside (Scheme 1), is an effective ingredient mainly extracts from the dry rhizome of Liliaceae plants *Smilax china* L.. *Smilax china* L. is a traditional Chinese medicine in common use, which exhibits remarkably anti-inflammatory analgesic, potent dispel rheumatism, diuresis, detumescence and antibiosis properties [1–4]. It is widely used in treating surgery acute infection, rheumatic arthritis, cancerology [5–7], and so on.

X. Peng · J. Yu · Q. Yu · H. Bian (✉) · F. Huang · H. Liang (✉)
College of Chemistry and Chemical Engineering,
Guangxi Normal University,
Guilin 541004 Guangxi Province, People's Republic of China
e-mail: gxnuchem312@yahoo.com.cn
e-mail: lianghongby@yahoo.com.cn

Serum albumin (SA) is a globular protein, which is the most abundant protein in the circulatory system and contribute about 80% osmotic pressure of blood [8–10]. It can transport many endogenous and exogenous substances, such as fatty acids, amino acids, steroids, metal ions and drugs, and modulate their delivery to cells in vitro and in vivo [11, 12]. The binding ability of drug to the serum albumin will affect the distribution and metabolism of drug in blood [13, 14]. So the research of the interaction between drugs and protein has important theoretical and practical significance in biochemistry and biomedicine.

In this paper, the binding constant, thermodynamic parameters and the major interaction force were analyzed by fluorescence spectroscopy. The synchronous fluorescence spectra and Raman spectroscopy indicated that the bound of ELN with BSA changed the conformation of protein. This study was performed under the simulated physiological conditions of pH=7.43.

Materials and Methods

Materials

Engeletin (99%, purchased from ICAMA) was dissolved in ethanol to prepare a stock solution of 1×10^{-3} mol·L^{-1}. 0.05 mol·L^{-1} phosphate buffer solution (PBS) of pH=7.43, contained 0.1 mol·L^{-1} NaCl. BSA (Sigma, molecular weight 66210) was dissolved in PBS to prepare stock solution of 1×10^{-3} mol·L^{-1} and stored at 4 °C, diluted before used. Ibuprofen and ketoprofen were dissolved in ethanol to prepare stock solution of 1×10^{-3} mol·L^{-1}, respectively. Sodium chloride, ethanol and other experimental drugs are analytically pure reagents. Double distilled water was used throughout.

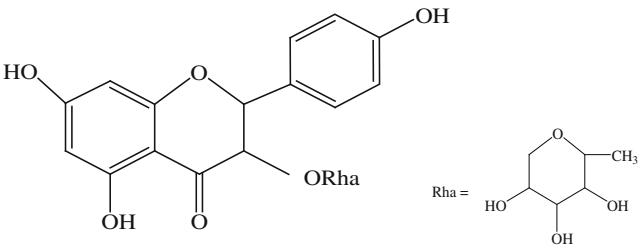

Scheme 1 The chemical structure of engeletin

UV–Visible Absorption Spectrum

The UV–Vis absorption spectra were measured on a Cary100 UV–Visible Spectrophotometer (Varian). Added a certain amount of 1×10^{-3} mol·L^{-1} ELN each time to 1.4×10^{-5} mol·L^{-1} BSA, the concentration of ELN was varied from 0 to 5×10^{-5} mol·L^{-1}, at a step of 1×10^{-5} mol·L^{-1}. Recorded the absorption difference spectra of BSA in the range of 190–450 nm with sample pool of 1 cm quartz absorption cell in the absence and presence of ELN.

Fluorescence Measurement

Fluorescence spectra were recorded by RF-5301 fluorescence spectrophotometer (Japan Shimadzu Company). Added a certain amount of 1×10^{-3} mol·L^{-1} ELN each time to 1.0×10^{-6} mol·L^{-1} BSA. Scan fluorescence spectra of BSA and fluorescence quenching spectra of BSA–ELN when the excitation wavelength was 280 nm. The slit width was 5/5 nm in the range of 300–500 nm.

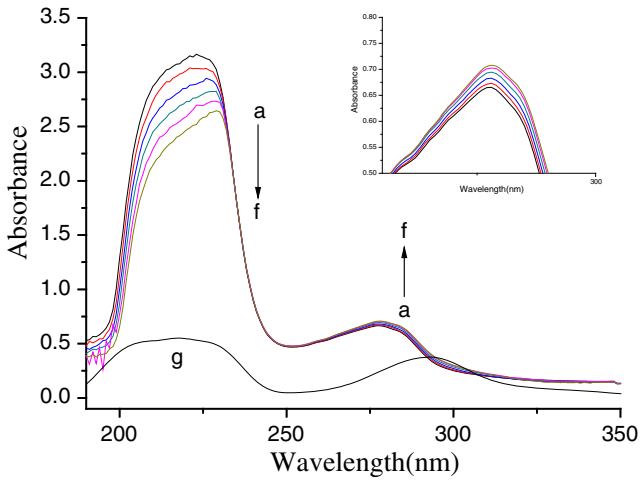

Fig. 1 Absorption difference spectra of BSA in the absence and presence of increasing amount of ELN. From a to f, the concentration of ELN was varied from 0 to 5×10^{-5} mol·L^{-1}, at a step of 1×10^{-5} mol·L^{-1}. g: absorption spectra of ELN of 5×10^{-5} mol·L^{-1}. Inset: the absorption difference spectra of BSA varied between 250 and 300 nm. [BSA]=1.4×10^{-5} mol·L^{-1}

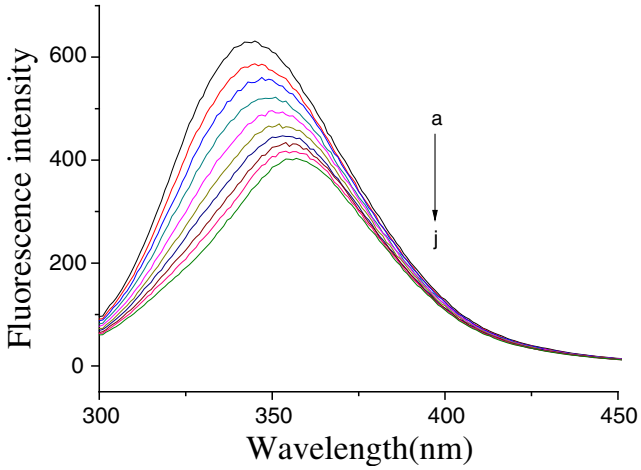

Fig. 2 Emission spectra of BSA in the absence and presence of ELN. From a to j, the concentration of ELN was varied from 0 to 22.5×10^{-6} mol·L^{-1}, at a step of 2.5×10^{-6} mol·L^{-1}. λ_{ex}=280 nm, pH=7.43, [BSA]=1.0×10^{-6} mol·L^{-1}

Fluorescence Decays Measurement

Lifetimes of fluorescence decay of BSA were performed on a Time-resolved Fluorescence spectrometer (Horiba Jobin Jvon Company, France) using Time Correlated Single Photon Counting (TCSPC) technique with a repetition rate of 1 MHz. The fluorescence decay curves were fit with a biexponential decay function.

Raman Spectrum

The Raman spectra were recorded on a Renishaw Invia +Plus FT–Raman spectrometer using an Ar^+ laser excitation with a wavelength of 514 nm. The laser power was 3 mW, and the recording range were 200–2,000 cm with a resolution of 1 cm^{-1}. Scan the Raman spectra of 0.5×10^{-3} mol·L^{-1} BSA and BSA–ELN system of the same

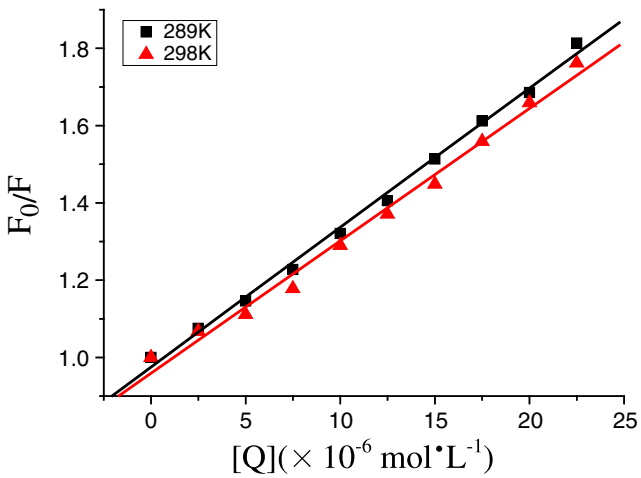

Fig. 3 The Stern–Volmer plots for the binding of ELN with BSA at different temperatures

Table 1 Stern–Volmer quenching constants for the interaction of ELN with BSA

T (K)	K_{SV} ($\times 10^4$ L mol^{-1})	k_q ($\times 10^{12}$ L mol^{-1} s^{-1})	R[a]	S.D.[b]
289	3.603	3.603	0.99804	0.01813
298	3.426	3.426	0.99490	0.02787

[a] R is the correlation coefficient

[b] S.D. is the standard deviation for the K_{SV} values

concentration under the temperature of 25 °C. The curve fitting of Raman spectral regions were analysed by the curve-fitting procedure (Peak Analyzer module of Origin 8.0, Microcal Origin, USA) using Gaussian curves.

Results and Discussion

The Analysis of UV–Visible Absorption Spectra

As showed in Fig. 1, the absorption difference spectra of BSA showed two maximum absorption wavelength (λ_{max}) around 223 and 278 nm, respectively. The increasing concentration of ELN caused the red shift of the peak at 223 nm to 229 nm and decreased the intensity of absorption. While the absorbance intensity of 278 nm increased 9.26% with unnoticeable change in the position. The absorption of BSA around 280 nm was mainly due to the tryptophan and tyrosine residues present in BSA [15], so the results obtained from Fig. 1 suggested that ELN interacted with the amino acid residues of BSA.

The Analysis of Fluorescence Spectra

In BSA, tryptophan, tyrosine and phenylalanine residues were the mainly fluorophores. Due to the effective intramolecular energy transfer effect between amino acid residues, we observed mainly tryptophan fluorescence [16]. Each BSA molecule had two tryptophan residues, located

Table 2 Lifetimes of fluorescence decay of BSA at different concentrations of ELN

[ELN] (μmol L^{-1})	Lifetime(ns)		Amplitude		$<\tau>$	χ^2
	τ_1	τ_2	A_1	A_2		
10	1.68	5.97	9.38	90.62	5.85	0.96
20	1.64	5.89	9	91	5.78	0.99
30	1.93	5.95	11.71	88.29	5.78	0.98
40	1.81	5.93	10.79	89.21	5.78	0.98
50	1.98	5.97	14.09	85.91	5.76	0.99
60	1.86	5.88	12.64	87.36	5.70	0.99

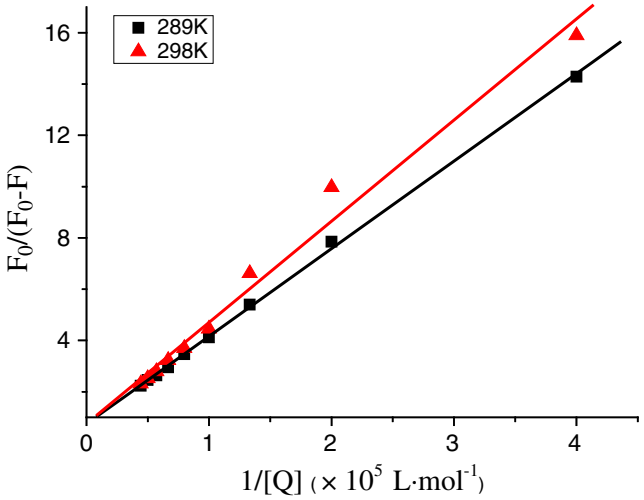

Fig. 4 The Lineweaver–Burk curves for the binding of ELN with BSA at different temperatures

Table 3 The static binding constants K and thermodynamic parameters of the BSA–ELN system at different temperatures

T (K)	K ($\times 10^4$ L mol^{-1})	R[a]	ΔG^0 (kJ mol^{-1})	ΔS^0 (J mol^{-1} K^{-1})	ΔH^0 (kJ mol^{-1})
289	2.191	0.99954	−24.00	47.27	−10.34
298	1.925	0.99147	−24.43		

[a] R is the correlation coefficient for the K values

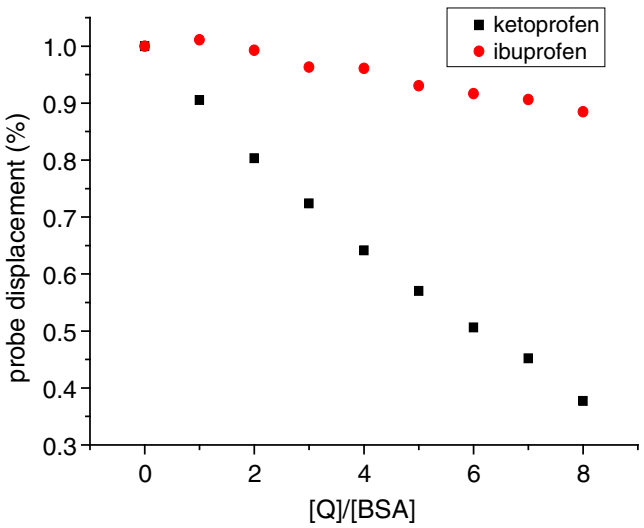

Fig. 5 Effect of site maker probe on the fluorescence of BSA–ELN. [BSA]=1.0×10^{-5} mol·L^{-1}, [ELN]=4.0×10^{-5} mol·L^{-1}. [Q]: ●, ibuprofen; ■, ketoprofen

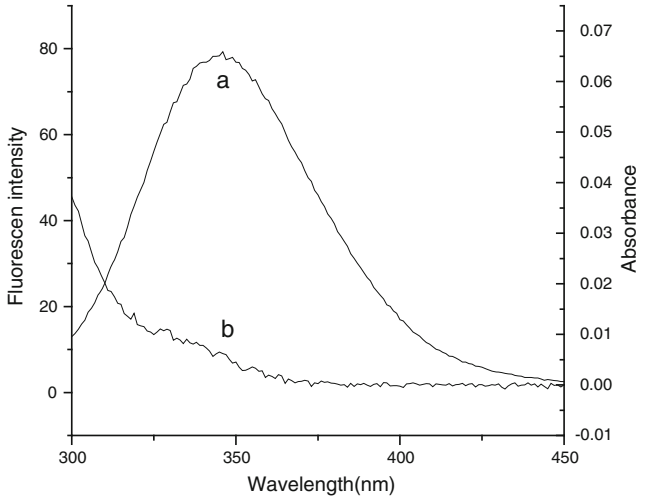

Fig. 6 The overlap of fluorescence spectra of BSA and the absorption spectra of ELN. (**a**) The fluorescence spectrum of BSA (1.0×10^{-6} mol L^{-1}); (**b**) The absorbance spectrum of ELN (1.0×10^{-6} mol·L^{-1})

in 134 and 212 respectively, and the fluorescence was mainly attributed to Trp–212 residues [17]. Figure 2 showed that the fluorescence intensity of BSA at 345 nm decreased regularly with the increasing of ELN. Significant spectral shift from 345 nm to 357 nm was observed, suggested that the polarity of the microenvironment around Trp–212 increased.

The quenching mechanism of fluorescence can be classified into static quenching and dynamic quenching [18]. The dynamic quenching depended on diffusion rate, thus increasing temperature will lead to the speeding up of diffusion and then increase the quenching rate constants. But for static quenching, increasing temperature will reduce the stability of the complex, so the effect was opposite [18, 19].

We used Stern–Volmer equation to analyze the fluorescence quenching [18]:

$$F_0/F = 1 + kq\tau_0[Q] = 1 + K_{SV}[Q] \quad (1)$$

where F_0 and F are the fluorescence intensity in the absence and presence of quencher, respectively. k_q is the quenching rate constant. τ_0 is the average fluorescence lifetime of the biomolecule in the absence of quencher. $[Q]$ is the concentration of quencher. K_{SV} is the Stern–Volmer quenching constant.

The Stern–Volmer plots for the binding of ELN with BSA at different temperatures were showed in Fig. 3. The K_{SV} values calculated from Stern–Volmer plots were listed in Table 1. If K_{SV} was the dynamic quenching constant, due to the fluorescence lifetime τ_0 of biological macromolecules was about 10^{-8} s [20], we obtained the quenching rate constant k_q. As showed in Table 1, k_q were much greater than 2.0×10^{10} L·mol^{-1}·s^{-1}, it proved that the bound of ELN to BSA was a static quenching process [21].

In order to further demonstrate the quenching mechanism, we measured the fluorescence lifetime of BSA. The results of the fluorescence decay of BSA in the absence and presence of ELN were listed in Table 2. The fluorescence lifetime of BSA almost remained the same with the increasing of ELN, which proved that the above process was static quenching [22].

The static quenching equation is presented by [19, 23]:

$$F_0/(F_0 - F) = 1/f + 1/(Kf[Q]) \quad (2)$$

Where f is the fraction of accessible fluorescence; K is the static binding constant of ELN with BSA, which can be

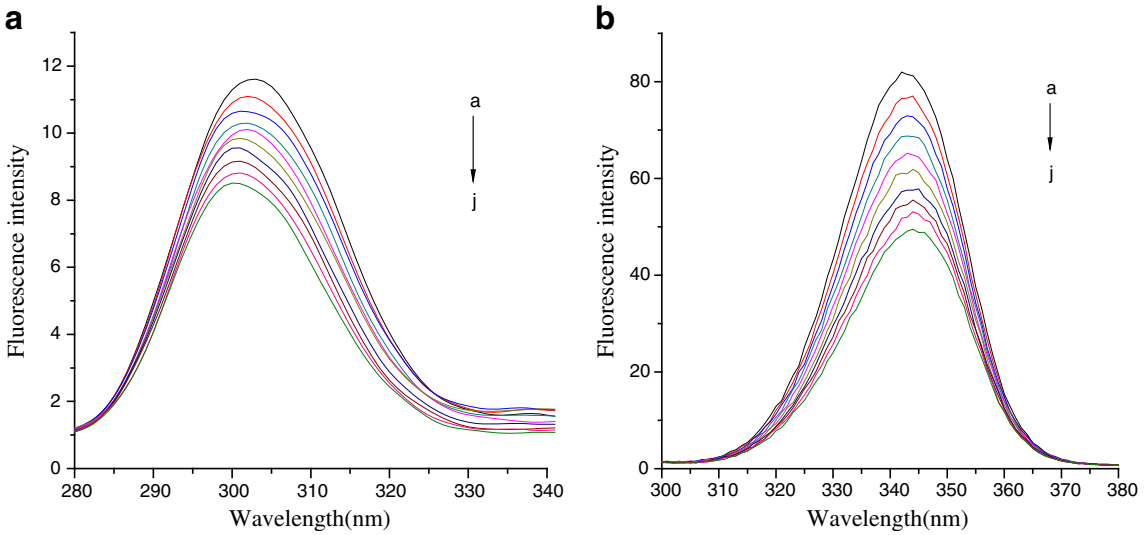

Fig. 7 The synchronous fluorescence spectra of BSA–ELN. (**a**) Δλ=15 nm; (**b**) Δλ=60 nm. [BSA]=1.0×10^{-6} mol·L^{-1}. From a to j, the concentration of ELN was varied from 0 to 9.0×10^{-6} mol·L^{-1}, at a step of 1.0×10^{-6} mol·L^{-1}

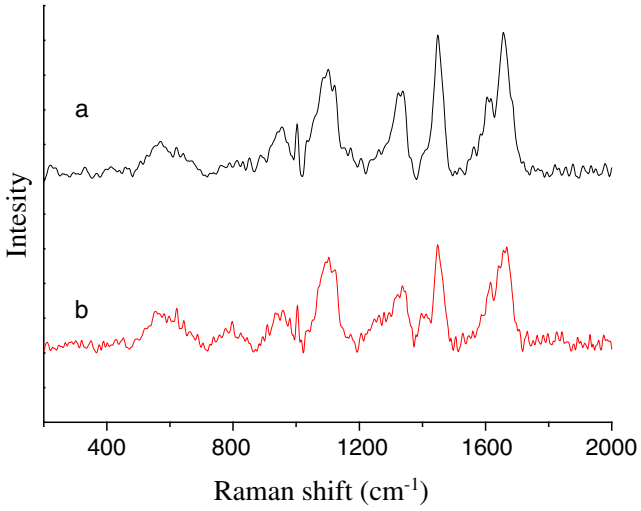

Fig. 8 Raman spectra of free BSA (**a**) and ELN–BSA system (**b**). [BSA]=0.5×10^{-3} mol·L^{-1}, the molar ratio of [ELN]/[BSA] is 1:1

determined by the slope and intercept of Lineweaver–Burk plots as showed in Fig. 4.

The static quenching was due to the formation of nonfluorescent or weakly fluorescent complexes between ELN and BSA, which will result in the decrease of binding constant with increasing temperature. The values of binding constant K were listed in Table 3. The results can further illustrated that the fluorescence quenching of BSA was static quenching [24].

Thermodynamic Parameters and the Nature of the Binding Forces

The acting forces between biomolecule and drug include hydrogen bond, van der Waals' force, electrostatic force and hydrophobic interaction, etc. [25]. The main thermodynamic parameters to determine the interactions between drugs and biomolecule are enthalpy change (ΔH^0) and entropy change (ΔS^0). If the change of temperature could be ignored, the enthalpy change was regarded as a constant, so Van't Hoff equation was used:

$$\ln K = -\Delta H^0/RT + \Delta S^0/R \tag{3}$$

$$\ln(\frac{K_2}{K_1}) = (\frac{1}{T_1} - \frac{1}{T_2})(\frac{\Delta H^0}{R}) \tag{4}$$

where ΔH^0 is the standard enthalpy change; ΔS^0 is the standard entropy change. The standard free energy change (ΔG^0) can be obtained from Gibbs–Helmholtz equation:

$$\Delta G^0 = \Delta H^0 - T\,\Delta S^0 = -RT\ln K \tag{5}$$

In this case, ΔH^0, ΔS^0 and ΔG^0 can be calculated according to Eqs. 4 and 5. The results were listed in Table 3. The negative value of ΔG^0 suggested that the reaction between ELN and BSA was spontaneous. The positive values of ΔS^0 were evidence of hydrophobic interactions [26]. According to Ross and Subramanian [27], the negative enthalpy (ΔH^0) and positive entropy (ΔS^0) values indicated that the main acting forces between ELN and BSA was hydrophobic interactions, but the hydrogen bond interactions cannot be excluded.

The Binding of Fluorescent Probes

According to the method presented by Sudlow et al., the following equation was used to determine the percentage of displacement of the probe [28]:

$$\text{probe displacement}\ (\%) = F_2/F_1 \times 100 \tag{6}$$

where F_1 and F_2 represent the fluorescence intensity of BSA–ELN system in the absence and presence of the probe, respectively. Figure 5 showed that the increasing concentration of ketoprofen decreased the fluorescence intensity of BSA–ELN system significantly, while the

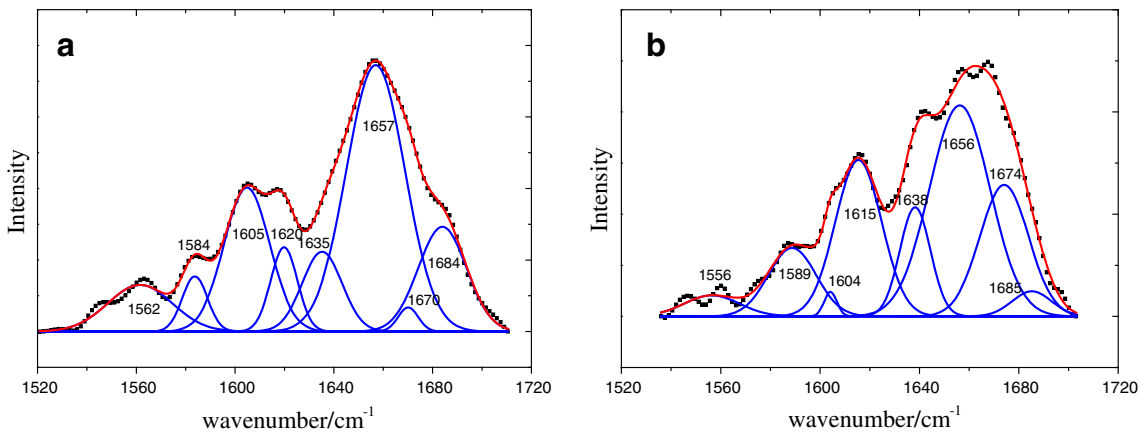

Fig. 9 The curve fitting of amide I of free BSA (**a**) and ELN–BSA (**b**) in buffer solution with [ELN]/[BSA]=1:1. [BSA]=0.5×10^{-3} mol·L^{-1}. The experimental spectrum (*black dots*), the fitting curve (*solid line*)

Table 4 The curve fitting results of Raman amide I of BSA

System	α–helix (%)	β–sheet (%)	β–turn (%)
BSA	64.22	15.05	20.73
BSA–ELN	54.39	41.47	4.14

Table 5 The conformation of the 17 disulfide bridges of BSA

System	g–g–g	g–g–t or t–g–g	t–g–t
BSA	5	6	6
BSA–ELN	1	7	9

fluorescence intensity didn't changed much in the case of ibuprofen. It suggested that ELN bound to the Site I of BSA [29].

Binding Distance between the ELN and BSA

According to Förster's non-radiative energy transfer theory [30], the rate of energy transfer depends on (i) the relative orientation of the donor and acceptor dipoles, (ii) the extent of overlap of fluorescence emission spectrum of the donor with the absorption spectrum of the acceptor and (iii) the distance between the donor and the acceptor. The efficiency of energy transfer E can be given by the following equation [31]:

$$E = 1 - \frac{F}{F_0} = \frac{{R_0}^6}{R_0^6 + r^6} \tag{7}$$

here r is the distance between acceptor and donor; R_0 is the critical distance in the case of the transfer efficiency is 50%, which can be determined by:

$$R_0^6 = 8.8 \times 10^{-25} K^2 n^{-4} \Phi J \tag{8}$$

where K^2 is the spatial orientation factor of the dipole; n is the refractive index of the medium; Φ is the fluorescence quantum yield of donor; J is the overlap integral of fluorescence emission spectrum of donor and absorption spectrum of acceptor:

$$J = \frac{\sum F(\lambda)\varepsilon(\lambda)\lambda^4 \Delta\lambda}{\sum F(\lambda)\Delta\lambda} \tag{9}$$

where $F(\lambda)$ is the fluorescence intensity of the donor at wavelength λ; $\varepsilon(\lambda)$ is the molar absorptivity of the acceptor at wavelength λ. Figure 6 was the overlap spectra of the fluorescence emission spectrum of BSA and absorption spectrum of ELN. The overlap integral J was calculated to be 7.4208×10^{-16} $cm^3 \cdot L \cdot mol^{-1}$. In this case, $K^2=2/3$, $\Phi=0.15$ and $n=1.36$ [32], so we found $R_0=1.64$ nm and $r=2.69$ nm, i. e. the distance between tryptophan residue in BSA and ELN was 2.69 nm. r was smaller than 7 nm, suggesting that the energy transfer from BSA to ELN occurred with high possibility [33].

Synchronous Fluorescence Spectra

The synchronous fluorescence spectra can provide information on the molecular microenvironment, particularly in the vicinity of the fluorophore functional groups [34]. When Δλ between the excitation and emission wavelengths was 15 or 60 nm, the synchronous fluorescence provided information for the tyrosine residues or tryptophan residues, respectively [35].

The synchronous fluorescence spectra of BSA–ELN were showed in Fig. 7. It was obvious that there was a blue shift of the maximum emission wavelength (λ_{max}) of tyrosine residues from 303 nm to 300 nm, while no obvious shift (from 343 to 344 nm) was observed at the λ_{max} of tryptophan residues. These results indicated a more hydrophobic environment around tyrosine, and a more polar environment around tryptophan residues due to the interaction of ELN with BSA [36, 37].

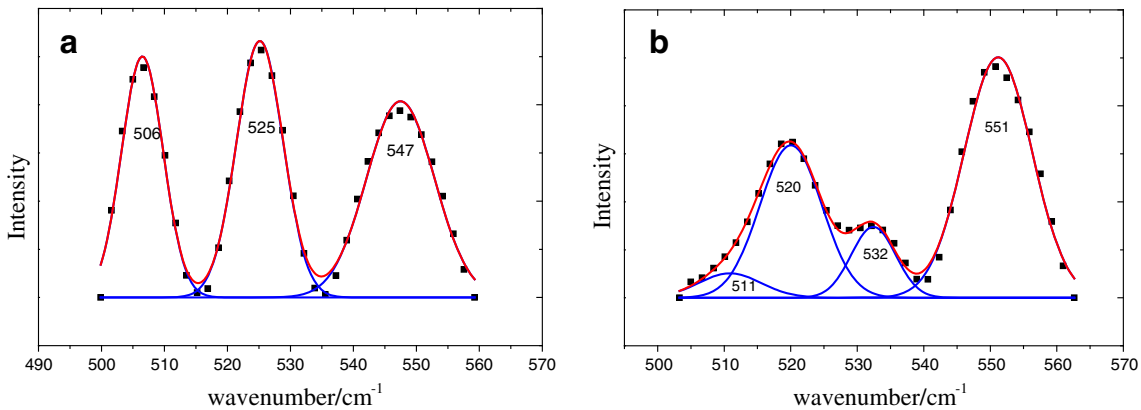

Fig. 10 Analysis of the S–S Raman band of free BSA (**a**) and BSA–ELN system (**b**). The experimental spectrum (*black dots*), the fitting curve (*solid line*)

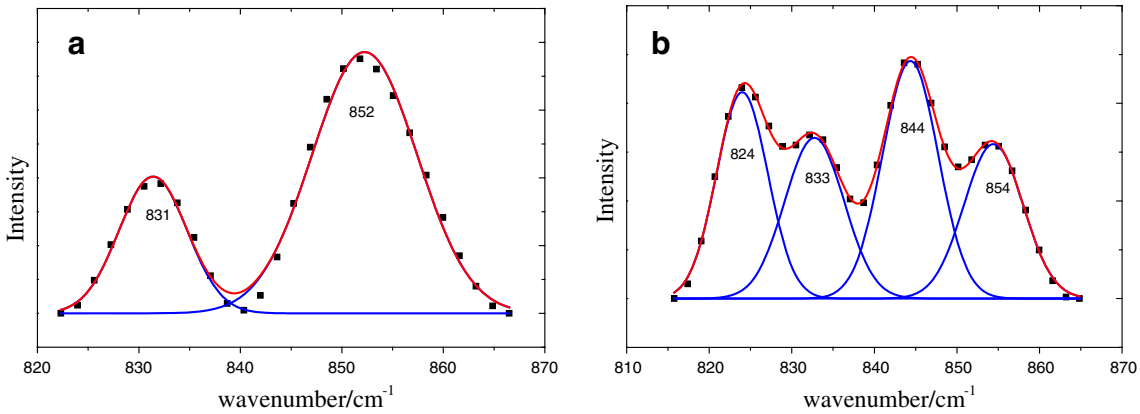

Fig. 11 Analysis of the Tyr side chains of free BSA (**a**) and BSA–ELN system (**b**): experimental spectrum (*black dots*), the fitting curve (*solid line*)

Raman Spectra

The Raman spectra of ELN–BSA and the curve fitting of Raman amide I were reported in Figs. 8 and 9. The peaks appeared in the region of 1,550–1,620 cm^{-1} were the ring vibration bands of aromatic residues [38]. The amide I band in the 1,630–1,700 cm^{-1} was due to the Raman–active vibrational modes of the CONH peptidic bond, i.e. C=O stretching weakly coupled to in–plane N–H bending [39]. The main peak around 1,655 cm^{-1} represented α–helix conformation [40, 41].

The curve fitting results were listed in Table 4. It suggested that the α–helix content decreased from 64.22% to 54.39%, while the content of β–sheet increased to 41.47%, the content of β–turn decreased to 4.14%, respectively.

Serum albumin contained 35 cysteine residues, they formed 17 disulfide bridges and one free cysteine residue. In Raman spectrum, the S–S stretching frequency was situated in the region of 500–550 cm^{-1}, it was sensitive to protein conformation [42, 43]. It has been determined that the peaks appeared around 510±5 cm^{-1} was belonged to the gauche–gauche–gauche (g–g–g) conformation, and the peaks around 525±5 cm^{-1} and 540±5 cm^{-1} were the features belonged to gauche–gauche–trans or trans–gauche–gauche (g–g–t or t–g–g), and trans–gauche–trans (t–g–t) conformations, respectively [44].

Figure 10 showed the curve fitting of S–S Raman bands in the region of 500–550 cm^{-1}. The conformations of the 17 disulfide bridges were presented in Table 5, which indicated that the binding of ELN to BSA induced the conformation change of four disulfide bridges.

To determine the environment of the Tyr residues, the relative intensity of the tyrosine doublet around 850 and 830 cm^{-1} was useful. The intensity ratio of I_{850}/I_{830} revealed the hydrogen bonding degree of the phenoxyl—OH group ("exposed" or "buried" Tyr) [45, 46]. According to the results showed in Fig. 11, the intensity ratio of I_{850}/I_{830} was 2.95 for free BSA, but it decreased to 0.96 after ELN was bound to BSA. The result suggested that the tyrosine residues were buried more in protein.

Figure 12 displayed the analysis of the Trp side chains. The intensity ratio of I_{1363}/I_{1340} decreased from 0.0779 to

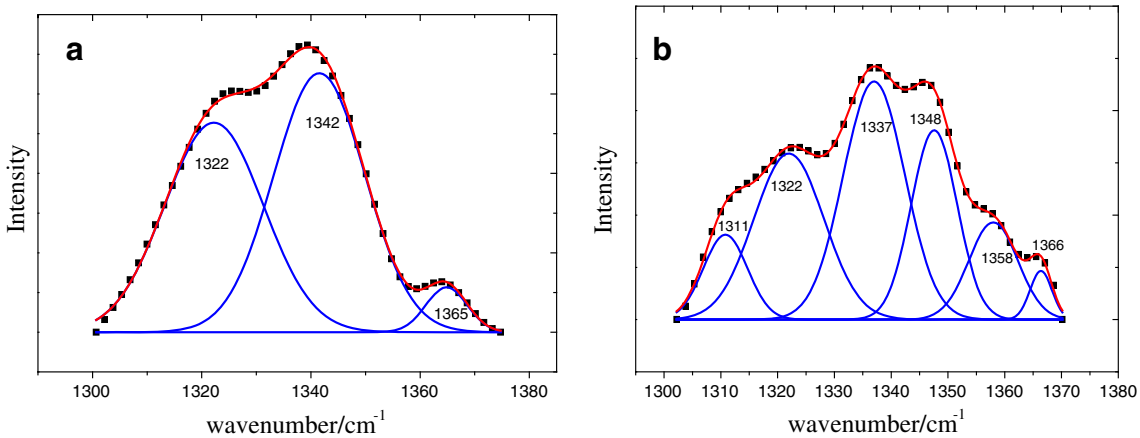

Fig. 12 Analysis of the Trp side chains of free BSA (**a**) and BSA–ELN system (**b**): experimental spectrum (*black dots*), the fitting curve (*solid line*)

0.0707 after the binding of ELN, indicating that the hydrophobicity of Trp environment decreased [47], which was in accord with the result of synchronous fluorescence spectra.

Conclusions

The interaction of ELN and BSA was studied by spectroscopic methods. The analysis of fluorescence illustrated that the bound of ELN to BSA was a static quenching process. The major interaction forces were hydrophobic and hydrogen bond interactions. ELN bound to the Site I of BSA with a distance of 2.69 nm. The conformation of BSA was changed by ELN binding with the decrease of α–helix content. As a result of the interaction between ELN and BSA, the exposedness of tyrosine residues and the hydrophobicity of Trp environment were both decreased. The binding of ELN also induced the conformational changes of disulfide bridges.

Acknowledgments This work was supported by the National Natural Science Foundation of China (Nos. 21061002, 20671023), Guangxi Natural Science Foundation of China (Nos. 2010GXNSFF013001, 2011GXNSFC018009) and the foundation of Key Laboratory for Chemistry and Molecular Engineering of Medicinal Resources.

References

1. Lin JY, Ye XL, Tang LX, Wu XJ, Cheng X (2010) Study on extracting technique for diosgenin from *Smilax*. Chin J Spectro Lab 27:2029–2031
2. Abdala S, Herrera DM, Benjumea D, Pe'rez P (2008) Diuretic activity of Smilax canariensis, an endemic Canary Island species. J Ethnopharmacol 119:12–16
3. Lu YN, Chen DS, Xu CH (2002) Study on the pharmacological action of *Smilax China* L. on promoting blood circulation to remove blood stasis. Chin J Hosp Pharm 22:538–540
4. Chen DS, Lu YN, Wang Q (2000) Anti-inflammatory action of *Smilax china* L. Chin J Hosp Pharm 20:544–545
5. Cox SD, Chamila K, Julie L (2005) Antioxidant activity in Australian native sarsaparilla (*Smilax* glyciphylla). J Ethnopharmacol 101:162–168
6. Xu SZ, Gan GP, Wu HZ, Wang GZ, Liu YW (2006) Investigation resource of medicinal plants of *Smilax* L. Res Pract Chin Med 20:26–28
7. Li YL, Gan GP, Zhang HZ, Wu HZ, Li CL, Huang YP, Liu YW, Liu JW (2007) A flavonoid glycoside isolated from *Smilax china* L. rhizome in vitro anticancer effects on human cancer cell lines. J Ethnopharmacol 113:115–124
8. Fei T, Ming G, Yu QS (2005) Studies on interaction between gatifloxacin and human serum albumin as well as effect of copper(II) on the reaction. Spectrochim Acta A 61:3006–3012
9. Guo YQ, Jian Q, Wei YL, Dong C (2007) Study on the interaction between tetrachloro tetrabromofluorescein and bovine serum albumins. J Anal sci 23:277–279
10. Carter DC, Ho JX (1994) Structure of serum albumin. Adv Protein Chem 45:153–204
11. Mathias U, Jung M (2007) Determination of drug–serum protein interactions via fluorescence polarization measurements. Anal Bioanal Chem 388:1147–1156
12. Yu ZL, Li DJ, Ji BM, Chen J (2008) Characterization of the binding of nevadensin to bovine serum albumin by optical spectroscopic technique. J Mol Struct 889:422–428
13. Rieutord A, Bourget P, Torche G, Zazzo JF (1995) In vitro study of the protein binding of fusidic acid: a contribution to the comprehension of its pharmacokinetic behaviour. Int J Pharm 119:57–61
14. Peters T (1996) All about albumin: biochemistry, genetics, and medical applications. Academic, San Diego, pp 76–131
15. Chakraborty B, Basu S (2009) Interaction of BSA with proflavin: a spectroscopic approach. J Lumin 129:34–39
16. Anbazhagan V, Renganathan R (2008) Study on the binding of 2,3-diazabicyclo[2.2.2]oct-2-ene with bovine serum albumin by fluorescence spectroscopy. J Lumin 128:1454–1458
17. Lakowicz JR (1983) Principles of fluorescence spectroscopy. Plenum Press, New York
18. Papadopoulou A, Green RJ, Frazier RA (2005) Interaction of flavonoids with bovine serum albumin: a fluorescence quenching study. J Agric Food Chem 53:158–163
19. Sun SF, Xiang GY, Hou HN, Liu Y (2006) Studies on interaction between 4-(4-Hydroxybut-2-ynyloxy)-3-(phenylsulfonyl)-1,2,5-oxadiazole-2-oxide and bovine serum albumin by spectroscopic method. Chin J Chem 24:1050–1053
20. Lakowicz JR, Weber G (1973) Quenching of fluorescence by oxygen. Probe for structural fluctuations in macromolecules. Biochem 12:4161–4170
21. Guo XJ, Zhang L, Sun XD, Han XW, Guo C, Kang PL (2009) Spectroscopic studies on the interaction between sodium ozagrel and bovine serum albumin. J Mol Struct 928:114–120
22. Naveenraj S, Anandan S, Kathiravan A, Renganathan R, Ashokkumar M (2010) The interaction of sonochemically synthesized gold nanoparticles with serum albumins. J Pharm Biomed Anal 53:804–810
23. Sułkowska A (2002) Interaction of drugs with bovine and human serum albumin. J Mol Struct 614:227–232
24. Cui FL, Kong XD, Qin LX, Zhang GS, Liu QF, Lei BL, Yao XJ (2009) Specific interaction of 4′-O-(a-l-Cladinosyl) daunorubicin with human serum albumin: the binding site II on HSA molecular using spectroscopy and modeling. J Photochem Photobiol B Biol 95:162–169
25. Hu YJ, Liu Y, Zhang LX, Zhao RM, Qu SS (2005) Studies of interaction between colchicine and bovine serum albumin by fluorescence quenching method. J Mol Struct 750:174–178
26. Ding F, Liu W, Zhang X, Zhang L, Sun Y (2010) Fluorescence and circular dichroism studies of conjugates between metsulfuron-methyl and human serum albumin. Colloids Surf B Biointerfaces 76:441–448
27. Ross PD, Subramanian S (1981) Thermodynamics of protein association reactions: forces contributing to stability. Biochem 20:3096–3102
28. Sudlow G, Birkett DJ, Wade DN (1992) Further characterization of specific drug binding sites on human serum albumin. Mol Pharmacol 12:1052–1061
29. He XM, Carter DC (1992) Atomic structure and chemistry of human serum albumin. Nature 358:209–215
30. Förster T (1966) In: Sinanoglu O (ed) Modern quantum chemistry, vol 3. Academic Press, New York, p 93
31. Sklar LA, Hudson BS, Simoni RD (1977) Conjugated polyene fatty acids as fluorescent probes: binding to bovine serum albumin. Biochem 16:5100–5108
32. Hu YJ, Liu Y, Zhao RM, Dong JX, Qu SS (2006) Spectroscopic studies on the interaction between methylene blue and bovine serum albumin. J Photochem Photobiol A: Chem 179:324–329

33. Valeur B, Brochon JC (2001) New trends in fluorescence spectroscopy. Springer Press, Berlin, p 25
34. Yue YY, Chen XG, Qin J, Yao XJ (2008) A study of the binding of C.I. Direct yellow 9 to human serum albumin using optical spectroscopy and molecular modeling. Dyes Pigm 79:176–182
35. Miller JN (1979) Recent advances in molecular luminescence analysis. Anal Proc 16:203–208
36. Lin H, Lan JF, Guan M, Sheng FL, Zhang HX (2009) Spectroscopic investigation of interaction between mangiferin and bovine serum albumin. Spectrochim Acta A 73:936–941
37. Xu H, Liu QW, Zuo Y, Bi Y, Gao SL (2009) Spectroscopic studies on the interaction of vitamin C with Bovine Serum Albumin. J Solution Chem 38:15–25
38. David C, Foley S, Mavon C, Enescu M (2008) Reductive unfolding of serum albumins uncovered by Raman spectroscopy. Biopolym 89:623–634
39. Jurasekova Z, Marconi G, Sanchez-Cortes S, Torreggiani A (2009) Spectroscopic and molecular modeling studies on the binding of the flavonoid luteolin and human serum albumin. Biopolym 91:917–927
40. Fabian H, Anzenbacher P (1993) New developments in Raman spectroscopy of biological systems. Vib Spectrosc 4:125–148
41. Iconomidou VA, Chryssikos DG, Gionis V, Pavlidis MA, Paipetis A, Hamodrakas SJ (2000) Secondary structure of chorion proteins of the teleostean fish *Dentex dentex* by ATR FT–IR and FT–Raman spectroscopy. J Struct Biol 132:112–122
42. Chuang VT, Kragh-Hansen U, Otagiri M (2002) Practical aspects of the ligand-binding and enzymatic properties of human serum albumin. Biol Pharm Bull 25:695–704
43. Sugeta H, Go A, Miyazawa T (1973) Vibrational spectra and molecular conformations of dialkyl disulfides. Bull Chem Soc Jpn 46:3407–3411
44. Van Wart HE, Lewis A, Scheraga HA, Saeva FD (1973) Disulfide bond dihedral angles from raman spectroscopy. Proc Natl Acad Sci USA 70:2619–2623
45. Tuma R (2005) Raman spectroscopy of proteins: from peptides to large assemblies. J Raman Spectrosc 36:307–319
46. Torreggiani A, Fagnano C, Fini G (1997) Involvement of lysine and tryptophan side-chains in the biotin—avidin interaction. J Raman Spectrosc 28:23–27
47. Miura T, Takeuchi H, Harada I (1988) Characterization of individual tryptophan side chains in proteins using Raman spectroscopy and hydrogen-deuterium exchange kinetics. Biochem 27:88–94